

# Observation of flux tube crossings in the solar wind

L. Arnold<sup>1</sup>, G. Li<sup>1,\*</sup>, X. Li<sup>1</sup>, Y. Yan<sup>2</sup>

<sup>1</sup> Department of Physics and CSPAR, University of Alabama in Huntsville 35899, USA,  
gang.li@uah.edu

<sup>2</sup> Key Laboratory of Solar Activity, National Astronomical Observatories of Chinese  
Academy of Sciences, Beijing 100012, China

Published: The Astrophysical Journal, 766, 2, 2013,

doi:10.1088/0004-637X/766/1/2

## ABSTRACT

Current sheets are ubiquitous in the solar wind. They are a major source of the solar wind MHD turbulence intermittency. They may result from non-linear interactions of the solar wind MHD turbulence or are the boundaries of flux tubes that originate from the solar surface. Some current sheets appear in pairs and are the boundaries of transient structures such as magnetic holes and reconnection exhausts, or the edges of pulsed Alfvén waves. For an individual current sheet, discerning whether it is a flux tube boundary or due to non-linear interactions, or the boundary of a transient structure is difficult. In this work, using data from the *Wind* spacecraft, we identify two three-current-sheet events. Detailed examination of these two events suggest that they are best explained by the flux tube crossing scenario. Our study provides a convincing evidence supporting the scenario that the solar wind consists of flux tubes where distinct plasmas reside.

## 1. Introduction

The solar wind provides a natural environment to study MHD turbulence in a collisionless plasma. Over the past few decades the launches of spacecraft such as Voyager, Helios, Ulysses, *Wind*, and ACE have made available a significant amount of data for analyzing the solar wind MHD turbulence.

The first theory of hydrodynamic turbulence, suggested by Kolmogorov (1941), known as the K41 theory, predicted a magnetic field power-law spectrum  $\sim k^{-5/3}$ . This  $-5/3$  exponent arises from the nonlinear interactions of the homogeneous hydrodynamic turbulence in which energy is cascaded from large scales to small scales. For incompressible MHD turbulence where the cascading process is mediated by counter-propagating Alfvén

wave packets, the Iroshnikov-Kraichnan (IK) theory (Iroshnikov 1964; Kraichnan 1965) and some recent theories of strong MHD turbulence (Boldyrev 2006; Boldyrev and Perez 2009) predict a power spectrum  $\sim k^{-3/2}$ .

One important concept in turbulence is intermittency. Ruzmaikin et al. (1995) suggested that intermittent structures can affect the solar wind MHD turbulence power spectrum. They pointed out that the effect of intermittency in the solar wind MHD turbulence is to reduce the exponent of the power law spectrum. Ruzmaikin et al. (1995) further suggested that intermittency is “in the form of ropes, sheets or more complicated fractal forms.” Recently, in studying current sheets (CS) in the solar wind, Li et al. (2011) found that the power spectrum of solar wind magnetic field behaves as K41 in periods that have abundant numbers of current sheets and behaves as IK in periods that are almost current-sheet free (see also Borovsky (2010)). Since these current sheets are a source of intermittency, the study of Li et al. (2011) supports Ruzmaikin et al. (1995).

A current sheet is a 2D structure across which the magnetic field direction changes abruptly. Current sheets can be of large scales. For example, the heliospheric current sheet and current sheets found in CME-driven shocks are all large scale current sheets. These are not the subjects of this study. Here we consider current sheets that are of small scales.

Some current sheets occur in pairs. These can be tangential discontinuities (TDs), often forming the two boundaries of a magnetic hole (see the review of Tsurutani et al. (2011) and references therein), or rotational discontinuities (RDs) which are the boundaries of an exhaust from a reconnection site (see (Gosling et al. 2005) and the review of Gosling (2011)). Comparing to magnetic holes, reconnection exhausts can be of larger scales. Gosling (2007) has found that the typical width of a reconnection exhaust is  $\sim 10^4$  km and some reconnection exhausts can be as wide as  $10^5$  km. Consequently, these boundaries may be practically identified as “single-current-sheet” event.

Most current sheets do not occur in pairs. These current sheets can be generated through non-linear interactions in the MHD turbulence (Zhou et al. 2004; Chang et al. 2004). Using ACE data, Vasquez et al. (2007) examined magnetic field discontinuities which can have very small spread angles for Bartels rotation 2286 (day 7 to 33 in 2001). They found that the statistical properties of these discontinuities form a single population and they are consistent with turbulence generated in-situ. By examining the probability density functions (PDF) of the magnetic field components from a 1D spectral code, Greco et al. (2008) showed that current sheets often occur at the super Gaussian tail of the PDF. Moreover, Greco et al. (2009) found that, at the inertial scale, in which the energy cascading rate is independent of the scale, the PDF of waiting times (WTs) between MHD discontinuities that are identified in the solar wind using the method of Tsurutani & Smith (1979) and those from MHD simulations are very similar, suggesting that these structures can be explained as a natural result of the non-linear interaction of the solar wind MHD turbulence.

Other opinions exist. In an earlier work, Bruno et al. (2001) studied current sheets in the solar wind by analyzing Helios 2 data using the minimum variance method to show how the magnetic field changed over selected time periods. Bruno et al. (2001) were the first to suggest that these structures may be boundaries between flux tubes. Borovsky (2008) analyzed an extended time period of magnetic field from the ACE spacecraft and examined the distribution of the spread angle across the current sheets. He showed that the angle distribution has two populations and suggested that the second population, dominating at large angles, could be “magnetic walls” and originate from the surface of the Sun. A solar wind that consists of many flux tubes can be viewed as a structured solar wind. In both the work of Bruno et al. (2001) and Borovsky (2008), the solar wind is envisioned to be full of structures, the flux tubes. Observed at a spacecraft, these structures are convected out with the solar wind. A similar scenario where structures convecting out from the Sun has

been proposed by Tu and Marsch (1991). Analysis on the cross helicity  $\sigma_c$  and residual energy  $\sigma_r$  by Bruno et al. (2007) supported the proposal of Tu and Marsch (1991).

Regardless the origin of a current sheet, Li (2008) developed a procedure to systematically identify these structures. Using this procedure, Li et al. (2008) examined current sheets in the solar wind and in the Earth’s magnetotail using *Cluster* magnetic field data and concluded that current sheets are more abundant in the solar wind. Later, Miao et al. (2011) examined over 3 years’ worth slow wind data using *Ulysses* observations and found there were 2 populations for the distribution of the spread angle across current sheets, in agreement with Borovsky (2008).

Perhaps a large fraction of current sheets identified in the solar wind are due to the non-linear interactions of the solar wind MHD turbulence, as shown in the work of Greco et al. (2008, 2009). However, a statistical study such as Greco et al. (2008, 2009) can not rule out the possibility that some current sheets in the solar wind are boundaries of flux tubes. Indeed, Borovsky (2008) has used plasma data including proton density and temperature, Helium abundance, electron strahl strength, etc. to identify possible plasma boundaries. Plasma data, however, is often of lower time resolution than magnetic field data. Furthermore, plasmas in different flux tubes may have similar properties except different velocities and magnetic field directions. Therefore, to unambiguously separate these two populations can be hard. Note, the occurrence rates of these two populations may have different radial dependence and/or different solar wind type dependence.

In this work, as an effort to identify flux tubes in the solar wind, we present a case study of two “triple-current-sheet” event using data from spacecraft *Wind*. A triple-current-sheet event is where three current sheets occurred in a relatively short period of time. The reason that we want to search for a triple-current-sheet event is the following. In the flux-tube scenario, the solar wind plasmas reside in different flux tubes and the solar wind magnetic

field and plasma properties differ in these flux tubes. Since flux tubes are 3D structures, we expect the boundary between two adjacent flux tubes to be curved and have small-scale ripples. This is shown in the cartoons in Figure 1. As these flux tubes are convected out past a spacecraft, depending on the relative configuration of the spacecraft trajectory and these ripples, one expects to observe most often a single crossing as in Figure 1 (a), and sometimes a double crossing as in Figure 1 (b), and occasionally a triple crossing as in Figure 1 (c). These three different cases are referred to as “single-current-sheet” events, “double-current-sheet” events, and “triple-current-sheet” events in this study.

A triple-current-sheet event can be used to discriminate between the scenario where current sheets are generated in-situ and the scenario where current sheets originate from the surface of the Sun. In the former case, one expects no correlations between these current sheets in the sense that plasmas before and after these current sheet crossings need not show any relationships. In the latter case, however, the spacecraft traverses through two distinct plasmas in the sequence of “I, II, I, II”, so the observed plasma properties do not vary arbitrarily.

## 2. Data Selection and Analysis

We use the 3 s plasma and magnetic field data from the 3DP (Lin et al. (1995)) and magnetic field (Lepping et al. (1995)) experiments on the *Wind* spacecraft. The data period was from September to October of 1995, which was during the declining phase of the solar cycle. It is ideal to select data in the solar minimum period due to lack of transient structures such as CMEs. For the data analysis method of current sheet identification, the readers are referred to Li (2008) and Miao et al. (2011).

In the following, we first present a single-current-sheet event and a double-current-sheet

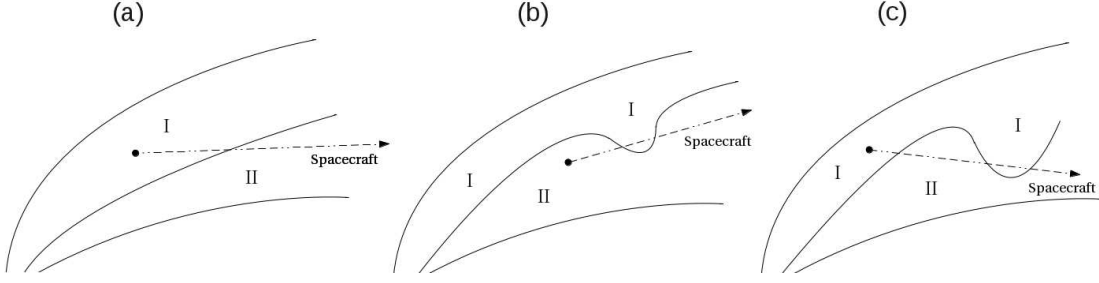


Fig. 1.— Cartoons illustrating (a) a single-current-sheet event, (b) a double-current-sheet event, and (c) a triple-current-sheet event. Note that in the case of triple-current-sheet event, the spacecraft traverses through two distinct plasmas in the sequence of “I, II, I, II”. Consequently, we expect to find the plasma properties to vary accordingly. Dashed line with arrow represents the relative trajectory of the *Wind* spacecraft passing through the flux tubes.

event. We then present two triple-current-sheet events.

Figure 2 is a single-current-sheet event which occurred on 1995-09-21. The current sheet in Figure 2 is located at 14:32 UT and is shown by the brown vertical line. Before the current sheet the magnetic field magnitude  $|B|$  decreases and the proton density  $N_p$  increases. In the scenario where a current sheet is the boundary of a flux tube, these changes across the current sheet occur because plasmas in different flux tubes have different properties (as shown in panel (a) of Figure 1). However, one need not invoke the flux-tube-crossing scenario to explain Figure 2. It can be simply a tangential discontinuity (TD) or one side of a reconnection exhaust. Indeed, careful examination shows that there was another small current sheet on  $\sim 14 : 32$  UT, when  $|B|$  decreased and  $N_p$  increased. Our selection procedure did not pick out this earlier current sheet.

The change across the current sheets are Alfvénic. The angle between  $\delta\vec{B}$  and  $\delta\vec{V}$  across the current sheet is  $7^\circ$ . For the earlier current sheet (that did not get picked up by our procedure), the angle is  $173^\circ$ . Such parallel and anti-parallel Alfvénic changes are always

associated with a reconnection exhaust (Gosling 2011). Furthermore, there was also a decrease of magnetic field and an increase of number density (but not temperature) between these two current sheets, providing another support for identification of a reconnection exhaust. Therefore, Figure 2, although identified as a single-current-sheet event using the Li (2008) algorithm, is really part of a pair of a bifurcated current sheet (Gosling et al. 2005; Gosling 2007, 2011).

Figure 3 is a double-current-sheet event. Two current sheets can be identified around 11:11:48 UT and 11:12:26 UT. In the scenario of flux-tube-crossing, Figure 3 can be understood as the spacecraft briefly crosses the magnetic wall between two flux tubes and then returns to the original flux tube. The schematic of this event is shown in the second panel of Figure 1. Note that the temperature decreases and the proton density increases between the two current sheets. As in Figure 2, although Figure 3 can be explained by the flux-tube-crossing scenario, it need not to be. The angles between  $\delta B$  and  $\delta V$  across the two current sheets are 175 and 167 degrees. Unlike the first event, this double-current-sheet is not associated with a reconnection exhaust. There was a slight but insignificant drop of the magnetic field magnitude, so it is unlikely to be a magnetic hole. The proton number density and proton temperature were also changed slightly at the two current sheets. These slight changes, together with the pulse-like changes of the 3 magnetic field components, suggest that this structure could be pulsed Alfvén wave (Gosling et al. 2011, 2012). Note, if this was a pulsed Alfvén wave, then according to Figure 3(a) of Gosling et al. (2012) and the fact that it has a duration of 46 seconds, it would be a long duration pulsed Alfvén wave.

Figure 4 and Figure 5 show two triple-current-sheet events that occurred on 1995-10-2 and 1995-10-13, respectively. Consider first the event shown in Figure 4. Throughout the event both  $B_y$  and  $V_y$  did not change much.  $B_x$  underwent a sharp change at 22:13:05 UT,



the first current sheet, after which it only changed slightly, until 22:25:00 UT when another sharp change occurred and  $B_x$  returned to values similar to those before 22:13:00 UT. At 22:25:00 UT at the third current sheet another sharp change in  $B_x$  occurred. After the crossing,  $B_x$  at and after 22:25:32 UT returned to a value comparable to  $B_x$  at 22:24:30 UT, just before crossing the 2nd current sheet. From the third panel, we can see that the  $V_x$  changes at the same times as  $B_x$ .

Similar behavior also occurred to  $B_z$  and  $V_z$ . Before crossing the first current sheet at 22:13:05 UT,  $B_z$  ( $V_z$ ) was almost a constant. After the crossing,  $B_z$  increased and  $V_z$  decreased.  $B_z$  also became slightly more turbulent. At the 2nd crossing at 22:25:00 UT,  $B_z$  and  $V_z$  changed back to almost the same value as before 22:13:00 UT. Then both  $B_z$  and  $V_z$  underwent another sudden change at the third current sheet crossing at 22:25:30 UT. After the third crossing,  $B_z$  returned to a value similar to that before the 2nd crossing at 22:25:00 UT.

The magnitude of the magnetic field  $|B|$  (the 2-nd panel), the proton number density  $N_p$  and the proton temperature  $T_p$  (the 4-th panel) did not vary much throughout the event. Before the crossing of the second current sheet, around 22:24:30 UT,  $|B|$  increased and  $N_p$  and  $T_p$  decreased. To better illustrate how the magnetic field direction evolves in this event, we have constructed an animation of the evolution of the unit magnetic field  $\hat{B}$ .

Two facts worth to note: 1) various plasma properties, including  $N_p$ ,  $T_p$  and the 3 components of  $\vec{B}$  and  $\vec{V}$  in the short period between 22:25:00 UT and 22:25:30 UT are very similar to those prior to 22:13:00 UT, suggesting that these are the same solar wind plasma. This can be clearly seen in the online animation. 2) similarly, the solar wind before and after the short period are likely the same and it is different from that in 1).

One may attempt to explain this triple-current-sheet event as the spacecraft crossing three uncorrelated individual current sheets that are generated by independent non-linear

interactions of the solar wind MHD turbulence. However, since independent current sheets have no correlations, the chance of the solar wind returning back to its original state after two independent current sheet crossings would be minute. Alternatively, one may argue that the plasma between 22:13:05 UT and 22:25:00 UT represented a rather long-lived transient structure, and interpret the first two current sheets as the boundaries of this structure. In such a case, one has to explain why after the third current sheet crossing, both the magnetic field and the plasma return to values the same as inside the transient structure.

Another triple-current-sheet event is the 1995-10-13 event, which is shown in Figure 5. Unlike the 1995-10-02 event, the 3-components of  $\vec{B}$  and  $\vec{V}$ , in particular,  $B_x$  and  $V_x$ , suffered some additional changes at and around the three current sheets, making the 1995-10-13 event less convincing than the 1995-10-02 event.

The first current sheet located at 19:32:28 UT. Both  $B_x$  and  $B_z$  showed a sudden jump across the first current sheet;  $V_x$  and  $V_z$  did not show significant changes.  $B_y$  and  $V_y$  also did not vary across the first current sheet. The current sheet is therefore non-Alfvénic. After crossing the first current sheet,  $B_z$  was almost a constant for the next  $\sim 7$  minutes until 19:39:40 UT, where the second current sheet was encountered. It increased across the second current sheet to a value similar to those prior to the crossing of the first current sheet. Comparing to  $B_z$ ,  $B_x$  was nearly constant after crossing the 1st current sheet for  $\sim 3$  minutes and then gradually increased until 19:39:00 UT, after which it increases noticeably before the second current sheet. Across the second current sheet, it dropped to a value similar to those prior to the crossing of the first current sheet. The third current sheet occurred at 19:40:15 UT. Across the third current sheet, there was a significant change of  $B_z$  and a small change of  $B_x$ . The two black horizontal dashed lines indicate that  $B_x$  ( $B_z$ ) before the first current sheet was similar to  $B_x$  ( $B_z$ ) between the second and the third

current sheets. The two magenta horizontal dashed lines indicate that  $B_x$  ( $B_z$ ) between the first and the second current sheets was similar to  $B_x$  ( $B_z$ ) after the third current sheet. Note that the change of  $B_x$  at the third current sheet was smaller than that at the second current sheet. After the third current sheet,  $B_x$  kept increasing, until 19:40:30 UT. The value of  $B_x$  after 19:40:30 UT is similar to those before 19:39:00 UT. As in the 1995-10-2 event, we also constructed an animation of the evolution of the unit magnetic field  $\hat{B}$  for this event.

For the 1995-10-02 event, the angles between  $\delta B$  and  $\delta V$  across the three current sheets are  $179^\circ$ ,  $176^\circ$ , and  $174^\circ$ , respectively. For the 1995-10-13 event, the angles between  $\delta B$  and  $\delta V$  are  $155^\circ$ ,  $124^\circ$  and  $173^\circ$ , respectively. While the three current sheets in the 1995-10-02 event are highly Alfvénic, those in the 1005-10-13 event are not.

### 3. Discussion and Summary

Current sheets are ubiquitous in the solar wind. They can be generated in-situ through non-linear interactions of the solar wind MHD turbulence (Greco et al. 2008, 2009), or represent the boundaries of flux tubes that originated at the Sun (Bruno et al. 2001; Borovsky 2008; Li et al. 2008). Appearing in pairs, they could also be the boundaries of reconnection exhausts ((Gosling 2011)).

An intriguing question one may ask is: for any particular current sheet, can we identify how it originated?

If current sheets that are generated in-situ and those that are convected out from the Sun have similar properties (such as the spread angles, the current sheet width, etc), then discriminating these two scenarios can be hard. However, as shown in the rightmost cartoon in Figure 1, the presence of triple-current-sheet event provides a strong support

to the flux-tube scenario. This is because in the flux-tube scenario the plasma and field changes across the three current sheets are intimately correlated: as the spacecraft crosses the three current sheets, the plasma before the first crossing and that between the 2nd and the 3rd crossing are the same; the plasma between the first and the second crossings and that after the third are the same. This is in stark contrast to the scenario where the current sheets are generated in-situ. In the latter scenario, the plasma changes at the three current sheets in a triple-current-sheet event need not match.

Note that the identification of a triple-current-sheet event does not tell us how many single-current-sheet events are due to flux-tube crossing. As discussed earlier, since a reconnection exhaust can be of large scale (Gosling 2007), some single-current-sheet events we identify can be the boundaries of reconnection exhausts. Gosling (2010) identified an occurrence rate of 40-80 reconnection events per month in solar minimum. In our study, we only consider current sheets which are abrupt (width  $< 10$  seconds) and whose spread angles are larger than  $45^\circ$ , we find about 350 “single-current-sheet” events per month. Assuming  $2 * 60 = 120$  are boundaries of reconnection exhausts, then the rest are presumably either generated in-situ or are the boundaries of flux tubes. Assuming 80% (50%) of the rest are generated in-situ, then one gets about 45 (115) single-current-sheet events that are flux-tube crossings per month.

If current sheets are boundaries of flux tubes that have a solar origin, e.g. super granules, then one may expect to find some statistical correlations between in-situ observations of current sheets and solar observation of super granules. Indeed, Bruno et al. (2001) have suggested that the sizes of the flux tubes, when tracing back to the solar surface, may correlate with the size of photospheric magnetic networks. In the work of Miao et al. (2011), using Ulysses observation, the distribution of the waiting time statistics of the current sheets were obtained. Assuming these flux tubes do not split or merge during

their propagation to 1 AU, then one may expect such waiting time statistics resembles the distribution of the magnetic network sizes. Examining the waiting time statistics of current sheet, and in particular, its dependence on heliocentric distance, and its correlation with supergranule size will be reported in future work.

To conclude, we have examined 2-month’s worth solar wind data from the *Wind* spacecraft and identified two triple-current-sheet events. The sequence of the observed magnetic field and plasma data in these two events are in agreement with the scenario where current sheets are flux tube boundaries, as depicted in Figure 1. Unambiguous identification of flux tubes in the solar wind is important because these structures present an additional source of solar wind MHD turbulence intermittency. They can affect the power spectrum of the solar wind MHD turbulence (Li et al. 2011, 2012) as well as affecting the transport of energetic particles in the solar wind (Qin and Li 2008).

We thank R.P. Lepping and R.P. Lin and the CDAWeb for making available the data used in this paper and the referee for very valuable suggestions. This work is supported in part by NSF grants ATM-0847719, AGS0962658, AGS1135432 and NASA grant NNH07ZDA001N-HGI and NNX07AL52A.

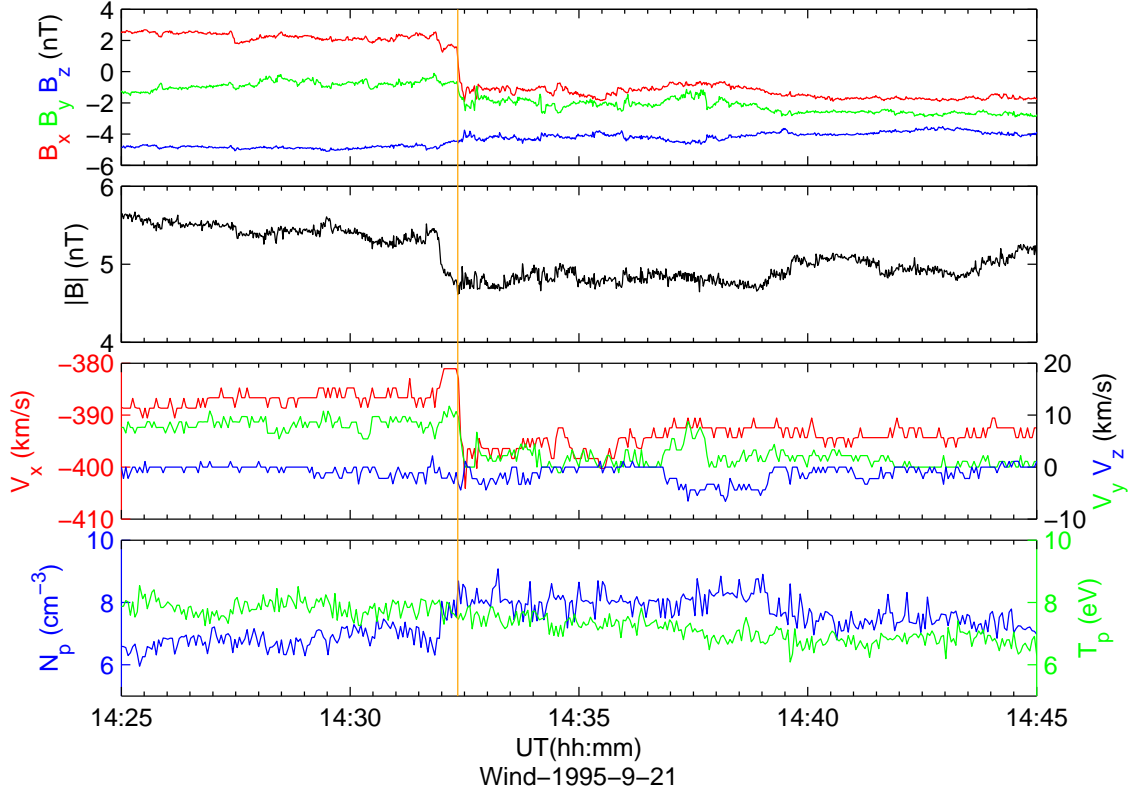


Fig. 2.— A single current sheet event occurred in 1995-09-21. Shown from top to bottom are the 3 components of the vector magnetic field in the Geocentric Solar Ecliptic (GSE) coordinate system, the magnitude of magnetic field, the 3 components of the vector proton velocity in the Geocentric Solar Ecliptic (GSE) coordinate system, and the solar wind proton number density and proton temperature, respectively. The brown vertical line marks the location of the current sheet.

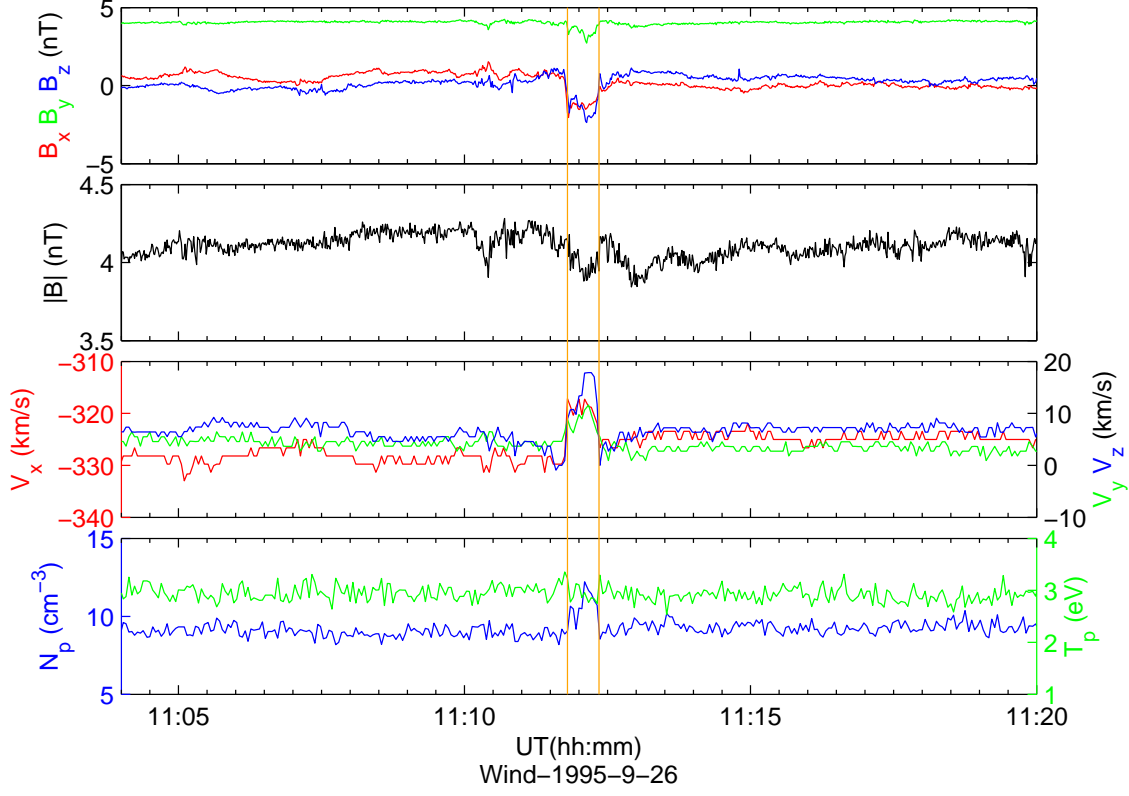


Fig. 3.— A double-current-sheet event that occurred in 1995-09-26. Shown from top to bottom are the 3 components of the vector magnetic field in the Geocentric Solar Ecliptic (GSE) coordinate system, the magnitude of magnetic field, the 3 components of the vector proton velocity in the Geocentric Solar Ecliptic (GSE) coordinate system, and the solar wind proton number density and proton temperature, respectively. The two brown vertical lines mark the location of the current sheet.

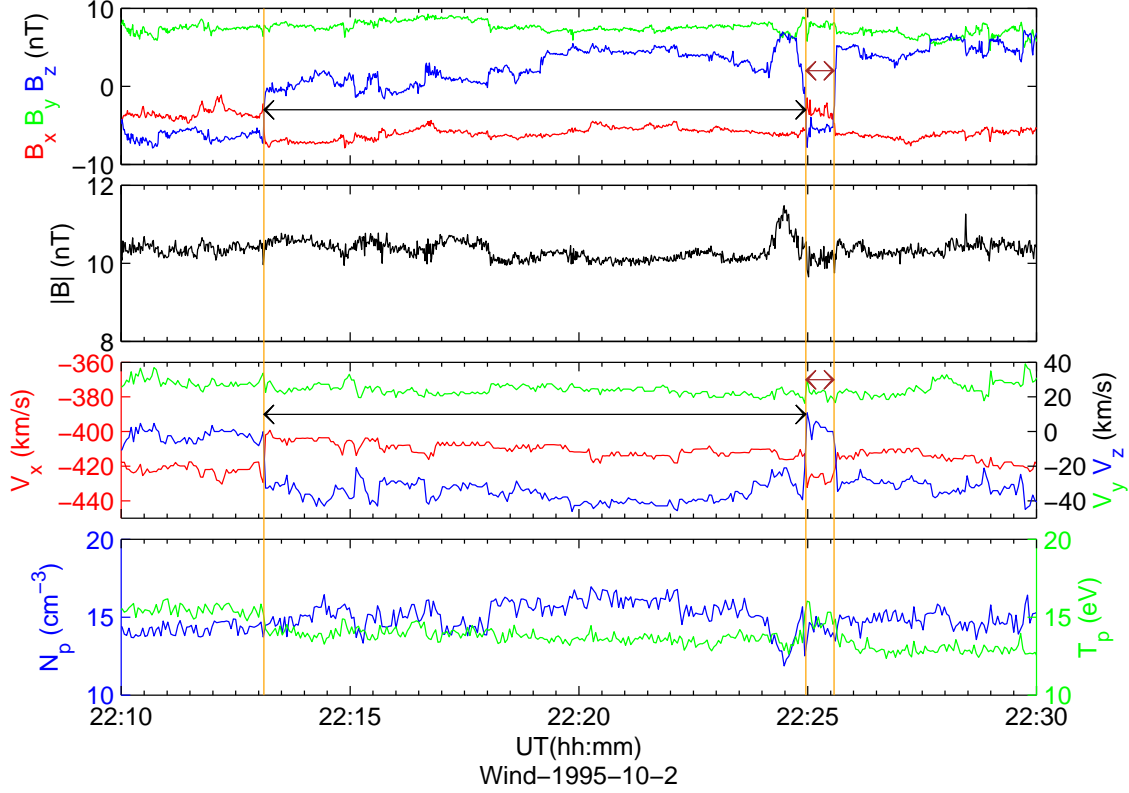


Fig. 4.— A triple-current-sheet event occurred on 1995-10-02. Shown from top to bottom are the 3 components of the vector magnetic field in the Geocentric Solar Ecliptic (GSE) coordinate system, the magnitude of magnetic field, the 3 components of the vector proton velocity in the Geocentric Solar Ecliptic (GSE) coordinate system, and the solar wind proton number density and proton temperature, respectively. The three vertical lines mark the location of the current sheet. Also see the online animation of the evolution of the unit magnetic field  $\hat{B}$  in this event.



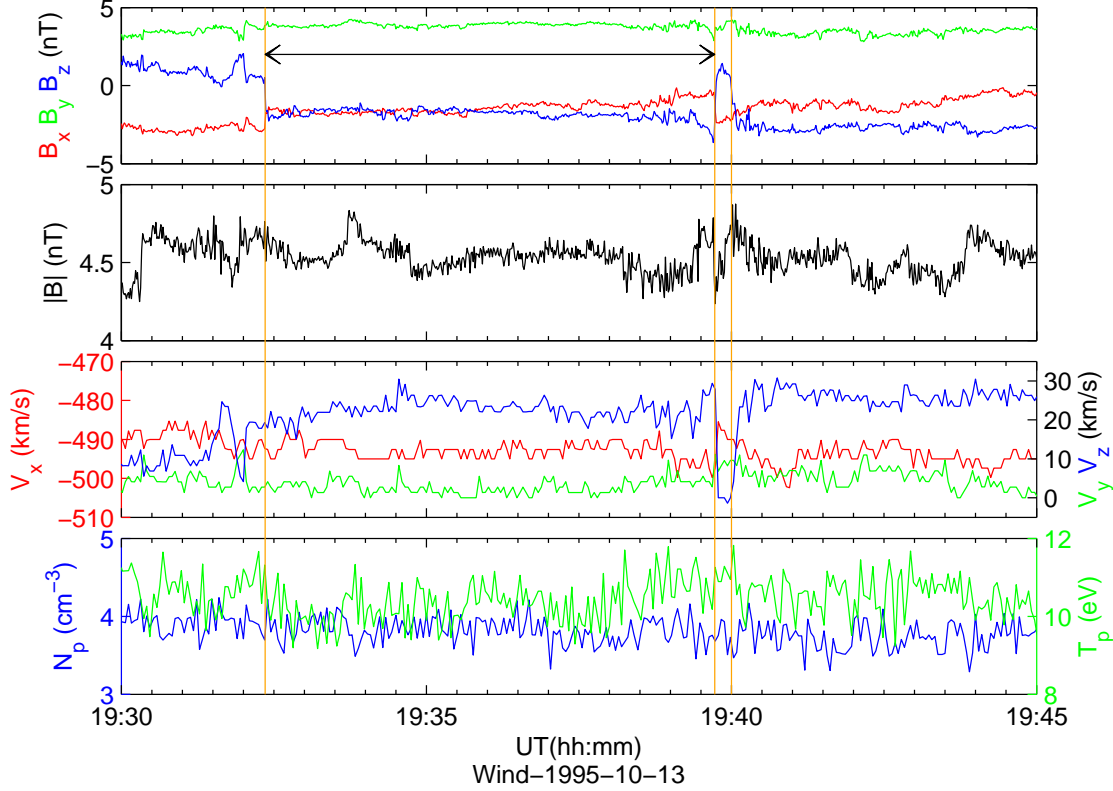


Fig. 5.— Same as Figure 4, but for the 1995-10-13 event. Shown from top to bottom are the 3 components of the vector magnetic field in the Geocentric Solar Ecliptic (GSE) coordinate system, the magnitude of magnetic field, the 3 components of the vector proton velocity in the Geocentric Solar Ecliptic (GSE) coordinate system, and the solar wind proton number density and proton temperature, respectively. The three vertical lines mark the location of the current sheet. Also see the online animation of the evolution of the unit magnetic field  $\hat{B}$  in this event.

## REFERENCES

- 274
- 275 Boldyrev, S., 2006, Phys. Rev. Lett. 96, 115002
- 276 Boldyrev, S., Perez, J., 2009, Phys. Rev. Lett. 103, 225001
- 277 Iroshnikov, P. S., 1964, Soviet Astronomy, 7, 566-571
- 278 Kolmogorov, A., 1941, C. R. Acad. Sci. URSS, 30, 301-305
- 279 Kraichnan, R. H., 1965, Phys. Fluids, 8, 1385-1387
- 280 Borovsky, J. E., 2008, J. Geophys. Res-Space Phys., 113, A08110, doi:10.1029/2007JA012684
- 281 Borovsky, J. E., 2010, Phys. Rev. Lett. 105, 111102
- 282 Bruno, R., Carbone, V., Veltri, P., Pietropaolo, E., Bavassano, B., 2001, Planet Space Sci.  
283 49 (12), 1201-1210
- 284 R. Bruno, R. D’Amicis, B. Bavassano, V. Carbone, and L. Sorriso-Valvo, 2007, Ann.  
285 Geophys., 25, 19131927
- 286 Chang, T., Tam, S., Wu, C., APR 2004. Phys. Plasmas 11 (4), 1287–1299.
- 287 Greco, A., Matthaeus, W. H., Servidio, S., Chuychai, P. and Dmitruk, P., 2009, The  
288 Astrophysical Journal Letters, 691, L111
- 289 Greco, A., P. Chuychai, W. H. Matthaeus, S. Servidio, and P. Dmitruk, 2008, Geophys.  
290 Res. Lett., 35, L19111, doi:10.1029/2008GL035454
- 291 Gosling, J. T., Skoug R. M., McComas, D. J., Smith, C.W., 2005, JGR, 110, A01107.
- 292 Gosling, J. T., 2007, ApJL, 671, L73.
- 293 Gosling, J. T., 2010, 12th Solar Wind Conference, AIP 1216, 188.

- 294 Gosling, J. T., 2011, Space Science Review, 10.1007/s11214-011-9747-2
- 295 Gosling, J. T., Tian, H., and Phan, T. D., 2011, ApJ, 737, L35
- 296 Gosling, J. T., Tian, H., and Phan, T. D., 2012, ApJ, 751, L22
- 297 Lepping, R. L., et al., 1995, Space Sci. Rev., 71, 207-229
- 298 Li, G., 2008, Astrophys. J. Lett. 672 (1), L65–L68
- 299 Li, G., Lee, E., Parks, G., 2008, Ann. Geophys., 26, 1889–1895
- 300 Li, G., Miao, B., Hu, Q., Qin, G., 2011, Phys. Rev. Lett. 106, 125001
- 301 Li, G., Qin, G., 2011, Hu, Q., and Miao, B., 2012, Adv. in Space Research, 49, p1327-1332,  
302 DOI: 10.1016/j.asr.2012.02.008
- 303 Lin, R. P., et al., 1995, Space Sci. Rev., 71, 125-153
- 304 Miao, B., Peng, B., Li, G., 2011, Annales Geophysicae 29 (2), 237–249
- 305 Qin, G. and Li, G., 2008, Astro. Phy. J., 682, L129-132. doi: 10.1086/591229
- 306 Ruzmaikin, A., Feynman, J., Goldstein, B., Smith, E., and Balogh, A., 1995, J. Geophys.  
307 Res-Space Phys., 100, 3395-3403
- 308 Tsurutani, B. T., and Smith, E. J., 1979, J. Geophys. Res-Space Phys., 84, 27733
- 309 Tsurutani, B. T., G. S. Lakhina, O. P. Verkhoglyadova, E. Echer, F. L. Guarnieri,  
310 Y. Narita, and D. O. Constantinescu, 2011, J. Geophys. Res., 116, A02103,  
311 doi:10.1029/2010JA015913.
- 312 Tu, C.-Y. and Marsch, E., 1991, Ann. Geophys., 9, 319332

- 313 Vasquez, B. J., V. I. Abramenko, D. K. Haggerty, and C. W. Smith, 2007, J. Geophys. Res.,  
314 112, A11102, doi:10.1029/2007JA012504
- 315 Zhou, Y., Matthaeus, W., Dmitruk, P., 2004, Phys. 76, 1015–1035